Journal of Photochemistry and Photobiology A: Chemistry 201 (2009) 8–14

Contents lists available at ScienceDirect

Journal of Photochemistry and Photobiology A: Chemistry

journal homepage: www.elsevier.com/locate/jphotochem

Photochromism of 2-benzyl-3-benzoyl-4(1*H*)-quinolone derivatives

V. Lokshin[a], N.A. Larina[a,b], O.A. Fedorova[b], A. Metelitsa[c], V. Khodorkovsky[a,*]

[a] *Interdisciplinary Center of Nanoscience CINaM (CNRS UPR 3118), 13288 Marseille Cedex 9, France*
[b] *Mendeleev University of Chemistry and Technology of Russia, 9, Miusskaya sq., Moscow, 125047, Russian Federation*
[c] *IPOC, Southern Federal University, Rostov on Don, 344090, Russian Federation*

ARTICLE INFO

Article history:
Received 26 June 2008
Received in revised form 24 August 2008
Accepted 5 September 2008
Available online 30 September 2008

Keywords:
Photochromism
Photoenolization
Quinolone

ABSTRACT

A series of 2-benzyl-3-benzoyl-4(1*H*)-quinolone derivatives was investigated. The UV–vis spectra of all photochromic derivatives and the corresponding colored photoenols are similar and almost solvent independent. In contrast, the stability of the photoenols depends strongly on the substituents at the quinolone moiety and solvent. We conclude that conversion of the photoinduced forms into the initial quinolones occurs through ionization rather than usual for photochromic compounds thermal relaxation or sigmatropic H-shift. The experimental observations are in good agreement with the results of quantum mechanical calculations.

© 2008 Elsevier B.V. All rights reserved.

1. Introduction

Photoenolization of *o*-alkylbenzophenones (**1**, Scheme 1) remains the focus of numerous studies [1] since it had been discovered in 1961 [2]. In a number of papers, the complex mechanism of this reaction was established and several short living intermediates, such as biradicals and geometrical isomers of photoenols (*o*-xylylenols) **2** were characterized [3–5]. Another intensively studied aspect of the rich chemistry of photoenolization involves the reactivity of **2**, which not only revert to the initial *o*-alkylbenzophenones presumably via 1,5-sigmatropic H-shift, but can also react with dienophiles [6-9], acylals [10], or undergo various intramolecular cyclizations [5,11].

In contrast, the potential of the *o*-alkylketone/photoenol couple as a photochromic system remains basically unexplored. The main obstacle for practical utilization of this system is the short lifetimes of the photoenols (up to several seconds for the *E*-isomers and less than 10^{-6} s. for the *Z*-isomers). At the same time, the possibility to increase the lifetimes of the both *E,E*- and *E,Z*- isomers of the photoenols by intramolecular hydrogen bonds up to several hours has been demonstrated more than 40 years ago on a series of 2-benzyl-3-benzoylchromones **3** (Scheme 1) and 2-benzyl-3-benzoyl-4(*1H*)-quinolones **4a** and **5a** [12] (Scheme 2). Recently, we demonstrated that further varying the structure of the quinolone derivatives affords a new type of photochemically reversible and thermally stable photochromes [13]. However, the scope and limitations of 2-benzyl-3-benzoyl-4(*1H*)-quinolones as potential photochromic compounds remain hitherto unexplored.

In order to gain deeper insight into the photochemistry of 2-benzyl-3-benzoyl-4(1*H*)-quinolone derivatives and behavior of the colored photo-induced forms, we prepared a series of differently substituted compounds, and report here on their spectroscopic and photochemical properties in solution along with the results of quantum mechanical calculations.

2. Experimental

2.1. Synthesis

2-Benzyl-3-benzoyl-4(1*H*)-quinolone **6**, the precursor of the parent compounds **4a** and **5a**, was prepared by a modified procedure [12], using phenyl benzoate as the acylation agent and Dowtherm A at the cyclization step.

A solution of ethyl 4-phenyl-3-phenylaminobut-2-enoate (2.8 g, 10 mmol) in 20 ml of freshly distilled DMF was added dropwise to a stirred suspension of NaH (0.72 g, 30 mmol) in 15 ml of DMF. After addition, stirring was continued for 4 h and a solution of phenyl benzoate (5.94 g, 30 mmol) in DMF was added dropwise. The resulting mixture was stirred for 20 h and then poured into 150 ml of cold water. The aqueous phase was acidified with 10% HCl till pH 4–5 and extracted with CH_2Cl_2 (3×30 ml). The combined extracts were washed with water, brine, dried by $MgSO_4$ and evaporated

* Corresponding author. Tel.: +33 4 91 82 93 22; fax: +33 4 91 82 93 01.
E-mail address: khodor@luminy.univ-mrs.fr (V. Khodorkovsky).

1010-6030/$ – see front matter © 2008 Elsevier B.V. All rights reserved.
doi:10.1016/j.jphotochem.2008.09.009

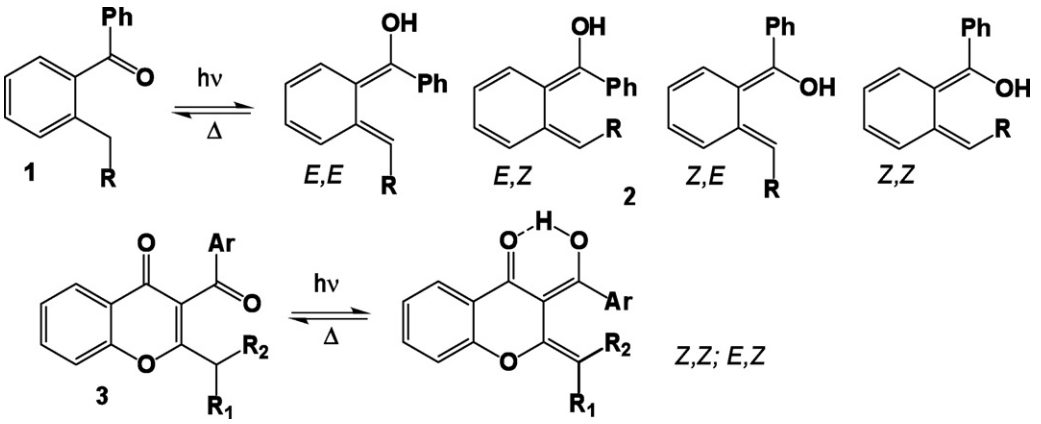

Scheme 1.

to give a crude acylated enaminone as a yellow oil, which without further purification was added dropwise under stirring to 100 ml of preheated to 230 °C Dowtherm A. The solution was refluxed for 20 min, allowed to cool down to room temperature and diluted with *n*-hexane. The precipitated gum crystallized upon addition of methanol. The beige solid was filtered, washed with methanol to give **6** (1.55 g, 46%). Analytical samples as colorless crystals, mp 254 °C (ref. [12]: 258–261 °C), were prepared by crystallization from methanol.

Derivatives **4a** and **5a** were obtained by methylation of **6** as described in [12]. Derivatives **4d**, **4e** and **4g** were prepared according to [14], previously unknown **4b** and **4c** were prepared analogously.

Derivative **4f** was prepared from **4d** by replacing one of the fluorine atoms with sodium methanolate and **4h** by thionation of **4e** using the Lawesson reagent. The ^{1}H and ^{13}C NMR spectra were recorded on a Bruker AC 250 spectrometer in $CDCl_3$, the δ values are given in ppm and J in Hz. The atom numbering is given in Scheme 2. The phenyl protons are indexed as primed for the benzoyl group, '*a*' for the benzyl group and '*b*' for the N-Ph group.

(**4b**): Yield 28%. mp 118–119 °C (colorless solid). ^{1}H NMR δ: 3.75 (2H, s, CH_2); 6.41 (1H, dd, J_{o1} = 8.7, J_{o2} = 8.7, H6); 6.70 (2H, m, H2b, H6b); 6.92 (3H, m, H3b–H5b); 7.10 (3H, m, H3′–H5′); 7.21–7.46 (7H, m, H2a′–H6a′, H7–H8); 8.00 (2H, m, H2′, H6′). ^{13}C NMR δ: 37.89 (CH_2); 110.78 (CH); 114.26 (CH); 116.11 (C); 125.56 (C); 126.89 (CH); 128.48 (CH); 128.69 (CH); 129.34 (CH); 130.10 (CH); 130.26 (CH); 132.59 (CH); 133.48 (CH); 135.98 (C); 137.75 (C); 138.03 (C); 145.10 (C); 150.32 (C); 162.08 (C); 175.37 (C(4)); 196.41 (C(3a)).

(**4c**): Yield 29%. mp 160–161 °C (colorless solid). ^{1}H NMR δ: 0.90 (3H, t, J = 7.3, CH_3); 1.51 (2H, m, CH_2); 3,91 (2H, t, J = 7.9, NCH_2); 4.01 (2H, s, CH_2); 7.25 (7H, m, H2a′–H6a′, H8, H6); 7.32 (2H, m, H3′, H5′); 7.53 (1H, m, H4′); 7.91 (2H, m, H2′, H6′); 8.41 (1H, dd, J_o = 6.9 J_m = 6.9, H5). ^{13}C NMR δ: 10.86 (CH_3); 21.74 (CH_2); 37.52 (CH_2); 48.90 (NCH_2); 102.47 (CH); 112.72 (CH); 123.56 (C); 124.56 (C); 127.36 (CH); 128.18 (2 CH); 128.58 (2 CH); 129.09 (2 CH); 129.42 (2 CH); 129.94 (CH); 133.42 (CH); 135.54 (C); 137.44 (C); 142.39 (C); 150.31 (C); 165.52 (C); 175.09 (C(4)); 196.53 (C(3a)).

(**4f**): Yield 93%. mp 142–143 °C (colorless solid). ^{1}H NMR δ: 0.90 (3H, t, J = 7.1, CH_3); 1.60 (2H, m, CH_2); 3.97 (5H, m, OCH_3, NCH_2); 4.06 (2H, s, CH_2 a); 6.80 (1H, d, J_m = 6.7, H8); 7.21–7.32 (5H, m, H2a′–H6a′); 7.42 (2H, m, H3′, H5′); 7.49 (1H, m, H4′); 7.88 (2H, m, H2′, H6′); 8.01 (1H, d, J_o = 11.3, H5). ^{13}C NMR δ: 10.96 (CH_3); 21.81 (CH_2); 37.44 (CH_2); 48.91 (NCH_2); 56.34 (OCH_3); 99.55 (CH); 122.16 (CH); 120.99 (C); 123.81 (C); 127.26 (CH); 128.10 (2 CH), 128.51 (CH); 129.04 (2 CH); 129.38 (2 CH); 133.31 (CH); 135.58 (C); 137.47 (C); 138.32 (C); 149.33 (C); 150.02 (C); 152.22 (C); 174.35 (C(4)); 196.69 (C(3a)).

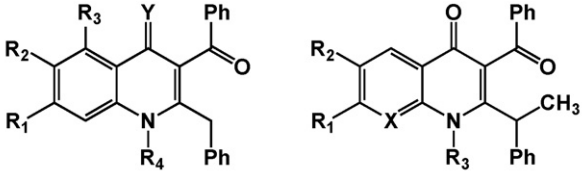

4	R_1	R_2	R_3	R_4	Y
a	H	H	H	Me	O
b	H	H	F	Ph	O
c	F	H	H	Pr	O
d	F	F	H	Pr	O
e	F	F	H	Ph	O
f	MeO	F	H	Ph	O
g	H	NO_2	H	Pr	O
h	F	F	H	Ph	S

5	R_1	R_2	R_3	X
a	H	H	Me	CH
b	F	H	Pr	CH
c	F	F	Pr	CH
d	F	F	Ph	CH
e	H	H	Ph	N

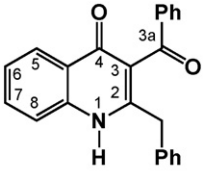

6

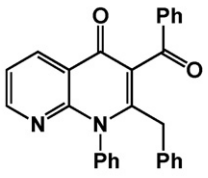

7

Scheme 2.

(**4h**): Yield 92%. mp 214–215 °C (orange solid). ^{1}H NMR δ: 3.60 (2H, s, CH_2); 6.49 (1H, dd, J_o = 11.5, J_m = 6.7, H8); 6.58 (1H, m, H4a′); 6.71 (2H, m, H2b, H6b); 7.00 (3H, m, H3b–H5b); 7.31 (2H, m, H2a′, H6a′); 7.42 (2H, m, H3a′, H5a′); 7.51 (3H, m, H3′–H5′); 8.00 (2H, m, H2′, H6′); 8.81 (1H, dd, J_o = 9.0, J_m = 9.0, H5). ^{13}C NMR δ: 37.98 (CH2); 107.09 (CH); 116.64 (CH); 126.97 (CH); 128.40 (CH); 128.75 (CH); 129.36 (CH); 130.22 (C); 130.41 (CH); 130.58 (C); 133.39 (CH); 134.99 (C); 135.63 (C); 136.65 (C); 137.08 (C); 143.75 (C); 149.52 (C); 153.73 (C); 191.50 (C(4)); 195.00 (C(3a)).

Derivatives **5b**, **5c**, **5d** and **5e** were prepared by C-methylation of **4c**, **4d**, **4e** and **7** [15] using the following general procedure.

A solution of 2-benzyl substituted quinolone (0.43 mmol) in dry DME (15 ml) was added to a stirred suspension of NaH (22 mg, 0.86 mmol) in dry DME (10 ml). The mixture was stirred at room temperature for 1 h, 4 ml of MeI was added, and the reaction mixture was refluxed for 1 h. The solvent was fully evaporated and the solid residue was dissolved in a mixture of 20 ml of CH_2Cl_2 and 20 ml of water. The organic phase was washed with a saturated solution of NH_4Cl (1 × 30 ml), brine (3 × 30 ml), dried with $MgSO_4$ and evaporated. The crude product was purified by column chromatography (silica gel, cyclohexane/ethyl acetate 7:3) to yield derivatives **5**. Crystallization from methanol afforded crystalline materials.

(**5b**): Yield 68%. mp 177–178 °C (colorless solid). ^{1}H NMR δ: 0.60 (3H, t, J = 7.3, CH_3); 1.50 (2H, m, CH_2); 1.72 (3H, d, J = 7.2, CH_3); 3,81 (2H, t, J = 7.6, NCH_2); 4.41 (1H, q, J = 7.2, CH); 7.19–7.33 (6H, m, H2a′– H6a′, H8); 7.40 (2H, m, H3′, H5′); 7,49 (1H, m, H4′); 7.88 (2H, m, H2′, H6′); 8.21 (1H, dd, J_o = 9.3, J_m = 9.3, H5). ^{13}C NMR δ: 10.74 (CH_3); 17.08 (CH_3); 27.09 (CH_2); 41.65 (NCH_2); 49.66 (CH); 102.91(CH); 112.78 (CH); 123.66 (C); 124.83 (C); 127.09 (CH); 127.34 (2 CH); 128.82 (2 CH); 129.16 (2 CH); 129.68 (2 CH); 129.92 (CH); 133.69 (CH); 137.46 (C); 139.95 (C); 142.94 (C); 155.03 (C); 161.26 (C); 175.74 (C(4)); 197.28 (C(3a)).

(**5c**): Yield 84%. mp 144–145 °C (colorless solid). ^{1}H NMR δ: 0.60 (3H, t, J = 7.2, CH_3); 1.50 (2H, m, CH_2); 1.70 (3H, d, J = 7.1, CH_3); 3.81 (2H, t, J = 7.7, NCH_2); 4.41 (1H, q, J = 7.1, CH); 7.02 (2H, m, H3a′, H5a′); 7.22–7.43 (7H, m, H2a′, H4a′, H6a′, H3′, H5′, H6, H8); 7.49 (1H, m, H4′); 7.98 (2H, m, H2′, H6′); 8.42 (1H, dd, J_o = 7.6, J_m = 7.6, H5). ^{13}C NMR δ: 10.42 (CH_3); 16.77 (CH_3); 21.07 (CH_2); 41.42 (NCH_2); 49.69 (CH); 105.43 (CH); 113.92 (CH); 123.73 (C); 124.01 (C); 126.73 (CH); 127.16 (2 CH); 128.57 (2 CH); 128.93 (2 CH); 129.39 (2 CH); 133.54 (C); 136.98 (C); 138.06 (C); 139.47 (C); 147.75 (C); 153.45 (C); 155.12 (C); 174.61 (C(4)); 196.68 (C(3a)).

(**5d**): Yield 61%. mp 218–219 °C (colorless solid). ^{1}H NMR δ: 1.61 (3H, d, J = 7.3, CH_3); 4.20 (1H, q, J = 7.3, CH); 6.33 (1H, dd, J_o = 12.6, J_m = 6.3, H8); 6.71 (2H, m, H2b, H6b); 6.92 (5H, m, H2a′–H6a′); 7.10–7.63 (8H, m, H2′–H6′, H3b–H5b); 8.14 (1H, dd, J_o = 9.9, J_m = 9.9, H5). ^{13}C NMR δ: 18.23 (CH_3); 41.36 (CH); 107.32 (CH); 113.37 (CH); 122.44 (C); 122.95 (C); 126.76 (CH); 128.13 (2 CH); 128.28 (2 CH); 129.22 (2 CH); 129.37 (2 CH); 129.44 (2 CH); 130.40 (CH); 130.68 (2 CH); 132.72 (CH); 136.84 (C); 138.19 (C); 138.78 (C); 139.99 (C); 147.98 (C); 152.95 (C); 156.82 (C); 175.24 (C(4)); 195.79 (C(3a)).

(**5e**): Yield 65%. mp 200–201 °C (colorless solid). ^{1}H NMR δ: 1.51 (3H, d, J = 7.1, CH_3); 4.10 (1H, q, J = 7.1, CH); 6.62 (1H, m, H4b); 6.70 (2H, m, H2b, H6b); 6.89 (2H, m, H3a′, H5a′); 7.00 (3H, m, H2a′, H4a′, H6a′); 7.17 (1H, dd, J_o = 7.9, J_o = 4.5, H6); 7.23–7.44 (7H, m, H2′–H6′, H3b, H5b); 8.40 (1H, dd, J_o = 4.2, J_m = 1.6, H7); 8.50 (1H, dd, J_o = 7.9, J_m = 1.6, H5). ^{13}C NMR δ: 18.54 (CH_3); 41.49 (CH); 120.47 (CH); 120.51 (C); 124.30 (C); 126.98 (CH); 128.08 (CH); 128.35 (CH); 128.78 (CH); 129.47 (CH); 129.58 (CH); 129.95 (CH); 132.90 (CH); 135.68 (CH); 137.01 (C); 138.83 (C); 139.00 (C); 152.49 (C); 153.05 (CH); 158.14 (C); 177.45 (C(4)); 196.05 (C(3a)).

All compounds gave satisfactory elemental analyses. The identity of derivatives **4a**, **5d** and **6** was additionally confirmed by X-ray structure determination [16].

2.2. Quantum mechanical calculations

Calculations were done using the Gaussian package [17]. The equilibrium geometries were optimized using the B3LYP 6-31G(d,p) method [18]. The energies are ZPE corrected. The electronic transition energies were calculated by the TD B3LYP 6-31G(d,p) method.

2.3. Photochemical measurements

UV–vis spectra were recorded using a Cary 50 spectrophotometer and processed by the MCR-ALS procedure [19]. Irradiation of derivatives **4** and **5** was carried out in degassed solutions using Oriel 150 W high pressure Xe lamp and Oriel 77250 monochromator.

3. Results

3.1. UV–vis absorption spectra of 2-benzyl-3-benzoyl-4(1H)-quinolones

All derivatives **4** and **5** (except **4g** and **4h**) exhibited the appearance of yellow to orange-red color upon irradiation of their solutions at the wavelengths corresponding to their absorption maxima. Surprisingly, the UV–vis absorption spectra of all photochromic compounds are practically independent of substituents at the quinolinone benzenic ring. Almost no solvatochromic shifts were observed when varying the solvent from cyclohexane to toluene and acetonitrile. Typical examples of the absorption spectra are shown in Fig. 1. The non-photochromic derivatives **4g** and **4h** are again the exceptions: whereas **4g** shows a monotonic increase in absorption down from 450 nm without a visible maximum, **4h** exhibits a weak absorption band about 500 nm along with the strong one at 420 nm. The common features of the photochromic compounds are the presence of a vibronically split band at around 320 nm (ε about 10,000–12,000, similar to the observed for the unsubstituted quinolone [20]) and a weak shoulder (ε < 10) at about 360 nm. Vibronically split bands corresponding to several overlapping electronic – vibronic transitions can be approximated by the Pekarian function [21,22].

Minimum four functions were required to achieve the fitting goodness better than 0.9 (Fig. 2). The four functions, of which three are of approximately the same area with the maxima at 344, 338 and 288 nm and the fourth one centered at 319 nm with the more than twice larger area, reproduce the shape of the experimental spectrum with the high precision. Very similar

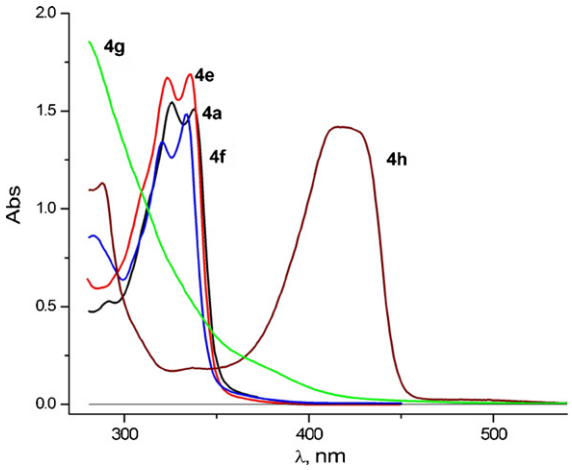

Fig. 1. UV–vis spectra of derivatives **4** in toluene.

Table 1
The deconvoluted experimental (in toluene) and calculated (in the gas phase) absorption spectra of **4a**.

λ_{max} experimental (nm)	λ_{max} calculated (nm)	Oscillator strength (f)	Major orbitals involved
344 (339)[a]	359	0.03	HOMO → LUMO ($\sigma,\pi \rightarrow \pi^*$)
338	330	0.04	HOMO^{-1} → LUMO; HOMO → LUMO ($\sigma,\pi \rightarrow \pi^*$)
319	309	0.08	HOMO^{-2} → LUMO; HOMO → LUMO^{+1} ($\sigma,\pi \rightarrow \pi^*$)
288	300	0.05	HOMO → LUMO^{+1} ($\sigma,\pi \rightarrow \pi^*$)

[a] In acetonitrile.

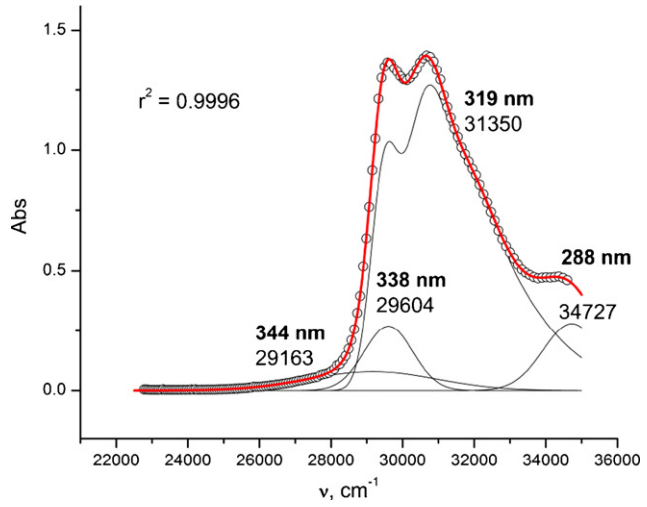

Fig. 2. Deconvolution of the absorption spectrum of **4a** (circles) by one Pekarian (31350 cm^{-1}) and three Gaussian (29163, 29604, 34727 cm^{-1}) functions.

results were obtained by fitting the spectrum of **4a** in acetonitrile, although the maximum of the lowest energy broad band was shifted from 344 nm to 339 nm. The negative solvatochromism of the first observed band (visible as a shoulder) suggests its interpretation as a C=O n → π* transition.

Quantum mechanical calculations can provide deeper insight into the nature of the observed spectroscopic features. Although the geometry optimization were done in the gas phase, the optimized equilibrium geometry of **4a** is very close to the experimental one found by the X-ray analysis [16]. In particular, the observed short intramolecular contact between the C-H fragment of the benzyl group and the oxygen atom of the benzoyl group (the C(H)···O distance 3.35 Å, that can be classified as the hydrogen bond [23]) is also reproduced. The calculated **4a** wavelengths of the first four transitions with the non-zero oscillator strength are given in Table 1.

The calculated excitation energies correspond very well to those obtained by deconvolution of the experimental spectra. Moreover, the calculated oscillator strengths are in reasonably good agreement with the areas of the functions used for deconvolution. The HOMO and HOMO^{-1} of **4a** are of the mixed σ,π-type involving the n orbitals of oxygen of the benzoyl C=O group (Fig. 3). One of these orbitals or both participate in all four transitions and the photochromic effect is indeed observed upon irradiation at any wavelength between 280 and 380 nm.

Analogous calculations were performed also for derivative **4h** using the same model chemistry and compared to the deconvoluted experimental spectrum. According to the calculation, the first longest wave absorption band at about 490 nm also corresponds to the HOMO-LUMO transition of $\sigma,\pi \rightarrow \pi^*$ type. However, the HOMO orbital is localized mostly on sulfur of the C=S bond and the next three higher energy transitions are of $\pi \rightarrow \pi^*$ type, accounting thus for the lack of photochromism.

3.2. Photochromic properties

The typical spectral changes occurring during irradiation of derivatives **4** and **5** are shown in Fig. 4. The photoenols generated from derivatives **4** absorb between 480 and 515 nm (orange-red coloration), whereas those generated from **5** absorb at shorter wavelengths (yellow coloration).

The initial photochemical investigation of **3** [24] as well as the ^{1}H NMR studies of **4d** showed that prolonged irradiation affords a complicated mixture of products, which stems from further photochemical conversions of the initially formed photoenols [25,26]. Therefore, the irradiation times were limited to 5–10 min. The presence of the isosbestic points indicates that during the relatively

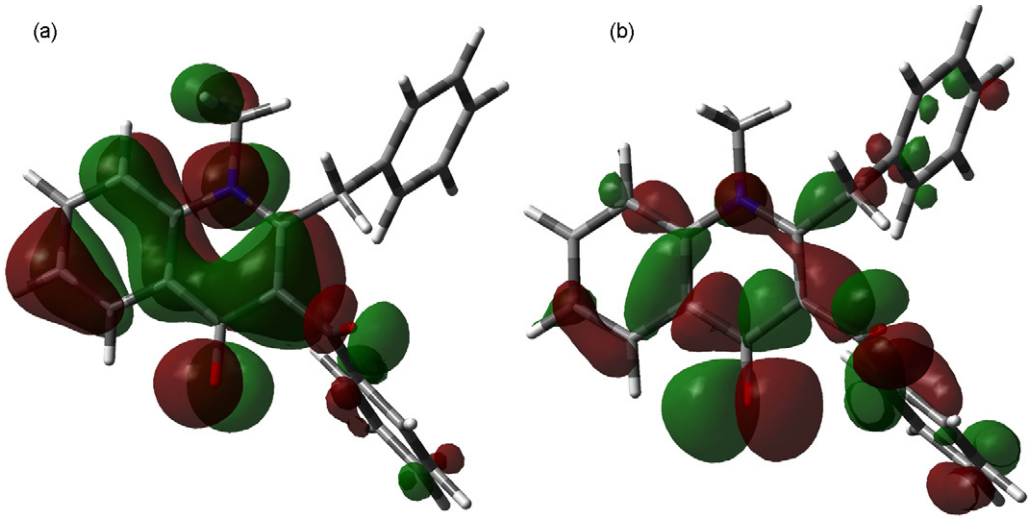

Fig. 3. (a) HOMO and (b) HOMO^{-1} of **4a**.

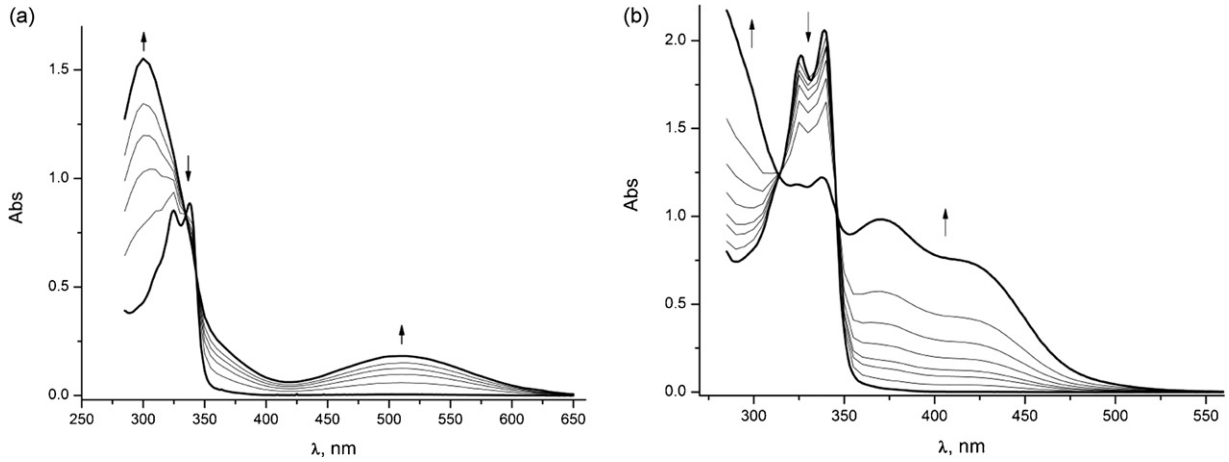

Fig. 4. Spectral changes upon irradiation of (a) **4e** and (b) **5d** in toluene.

Table 2
The deconvoluted experimental (in toluene) and calculated (in the gas phase) absorption spectra of the photoenol generated from **4e** (**8e** or **8e′**).

λ_{max} experimental (nm)	λ_{max} calculated (nm)	Oscillator strength (*f*)	Major orbitals involved
482	490	0.09	HOMO → LUMO ($\pi \rightarrow \pi^*$)
358	357	0.07	$HOMO^{-1}$ → LUMO ($\pi \rightarrow \pi^*$)
340	334	0.09	HOMO → $LUMO^{+1}$ ($\pi \rightarrow \pi^*$)
327	323	0.05	HOMO → $LUMO^{+2}$ ($\pi \rightarrow \pi^*$) $HOMO^{-4}$ → LUMO ($\pi \rightarrow \pi^*$)
312	315	0.20	HOMO → $LUMO^{+2}$ ($\pi \rightarrow \pi^*$)

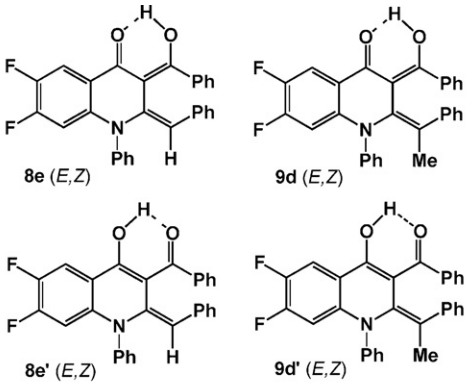

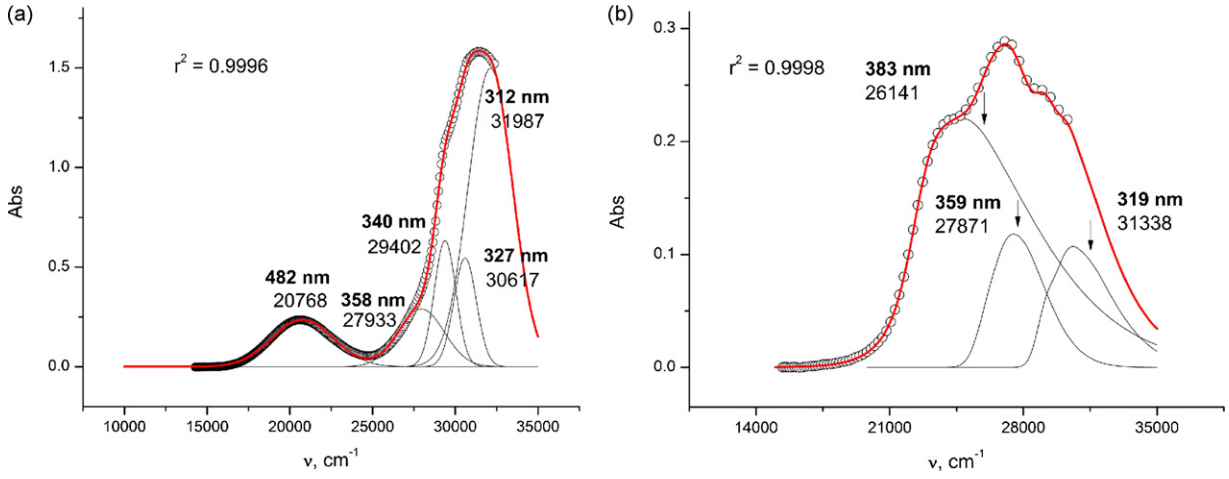

Fig. 5. Deconvolution of the absorption spectra of photoenols (circles) generated from (a) **4e** by five Gaussian and (b) **5d** by three Pekarian functions.

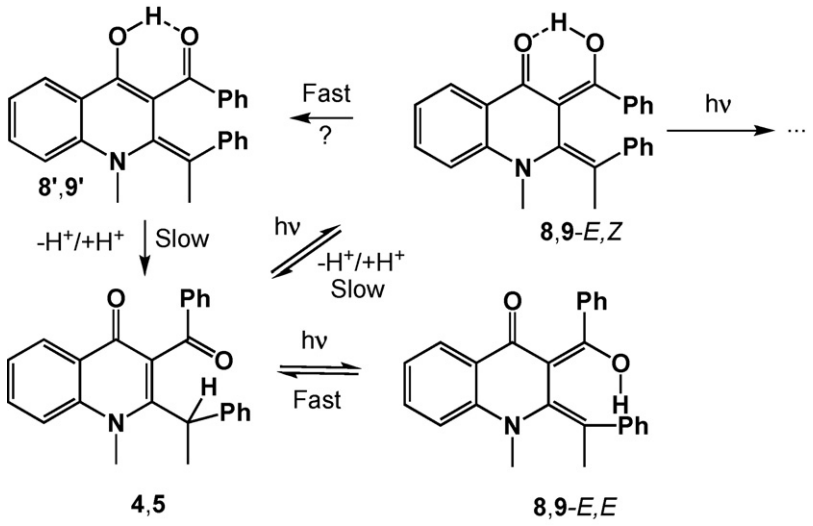

Scheme 3.

short irradiation times using the monochromatic light source, only a one-step photochemical reaction occurs. The isosbestic points gradually disappear when the irradiation time exceeds 8–12 min. The spectra sets were processed using the PCA and MCR [19,27] procedures, to confirm that during the initial stages of irradiation (as shown in Fig. 4) only two components (the starting material and a photoenol) were present in the solution, and allowed reconstruction of the photoproduct absorption spectra shapes (Fig. 5). The exclusive formation of the *Z,E* isomer of the photoenol at the initial stages of irradiation of **4d** has also been confirmed by the NMR spectroscopy [25]. In spite of the seemingly simple shape of the spectrum of the photoproduct generated from **4e**, deconvolution of the spectrum required five Gaussian spectral functions (Fig. 5). The results of the spectra calculations on the assumed photoenol structures **8e** (*E,Z*-isomer) (Table 2) and **9d** (*E,Z*-isomer) are also in excellent agreement with the experiment. However, practically the same spectra were predicted for the alternative photoenol structures **8e′** and **9d′**, which are more stable by 1–2 kcal/mol.

The stabilities of the colored photoenols depend strongly on solvent polarity. Whereas coloration in toluene persists during several days, it disappears in a few dozen of minutes in acetonitrile. The rate of discoloration depends also on the substituents. Quantitatively, the kinetics of discoloration can be characterized by the corresponding rate constants given in Table 3. Apparently, accepting substituents in the quinolinone benzenic ring and the phenyl group at the nitrogen atom substantially increase the discoloration rate by enhancing acidities of the photoenols. The same effect has the presence of the basic pyridine moiety (**5e**), which may catalyze proton transfer from the OH group to the CH group. On the contrary, replacing one of the electron accepting F substituent by the electron donating MeO group slows down discoloration about three times (**4d** vs. **4f**).

Table 3
The discoloration rate constants of derivatives **4** and **5** in acetonitrile.

Compound	$k_0 \times 10^{-2}$ (s^{-1})
4a	0.26
4b	0.49
4c	0.94
4d	1.56
4e	2.17
4f	0.48
5a	0.12
5b	0.18
5c	0.37
5d	0.31
5e	0.72

4. Discussion

Irradiation of derivatives **4** and **5** in solution and subsequent dark discoloration involves several processes that can be summarized as shown in Scheme 3.The triplet biradical intermediate formed upon irradiation [28] relaxes into a mixture of **8**(**9**)-*E,Z* and *E,E* isomers. Whereas the *Z,E* isomer may also form, both the *Z,E* and *E,E* isomers revert rapidly into the initial quinolone derivative. The *E,Z*-isomer is more stable than the Z,Z-isomer (see below) and is thus the only product that can be detected in our experiments. Its identity has been confirmed by the ^{1}H NMR spectra [25]. It is possible, however, that this isomer stabilizes further by rapid conversion into enols **8′** and **9′**. The formation of enols **8′** and **9′** directly from the triplet biradical intermediate cannot be excluded as well. Neither of enols **8**, **9**, **8′** and **9′** can interconvert into the initial quinolone derivative directly by thermal relaxation, as it happens with the majority of the photoinduced forms of known photochromic compounds. Conversion into the quinolinone derivatives can be achieved by ionization, as the enols are relatively strong acids. This consideration is supported by the above-mentioned strong dependence of the colored form lifetimes on polarity of solvents. Moreover, acceleration of the fading process in the presence of bases and inhibition by acids have been noticed already during the initial studies [12]. Our quantum mechanical calculations also support this interpretation. Thus, a comparison of the total electronic energies (ZPE corrected) showed that **4a** is more stable than its *Z,E* and *E,E* photoenol isomers by 21 kcal/mol and more stable than the *E,Z* and *Z,Z* photoenol isomers by 9.5 and 8 kcal/mol, respectively. The calculated gas phase proton affinities of the corresponding conjugate anion are 354 (the formation of **8a**-*E,Z*), 356 (the formation of **8a′**) and 362 kcal/mol (the formation of **4a**). These values can be compared to the calculated at the same level of theory proton affinities of monomeric benzoic and acetic acids: 356 and 366 kcal/mol, respectively.

5. Conclusions

The photochromic behavior of 2-benzyl-3-benzoyl-4(*1H*)-quinolones is characterized by the remarkable insensitivity of their absorption spectra to the substituent and solvent effects.

The color of the corresponding photoenols is predetermined by the substituent at 2-position: derivatives **4** featuring the 2-benzyl group provide orange-red coloration, corresponding to absorption at about 500 nm and derivatives **5** with the 2-benzylmethyl group give yellow color as the absorption band between 350 and 500 nm is developing. However, unlike the fading mechanism observed in the majority of the known photochromes, discoloration of the photogenerated species involves ionization of the strongly acidic photoenols and their stabilities are strongly dependent on both substituents and solvent. This feature offers the possibility to control the color by variation of pH (by an independent photochemical process or electrochemically) or by using specially designed organized media.

Acknowledgements

N.A.L. is thankful for the PhD fellowship to the "Reseau Formation-Recherche Franco-Russe" of the French Ministry for Education and Research.

References

[1] P.J. Wagner, in: W. Horspool, F. Lenci (Eds.), CRC Handbook of Organic Photochemistry and Photobiology, 2nd ed., CRC Press, 2004 (Chapter 58).
[2] N.C. Yang, C. Rivas, J. Am. Chem. Soc. 82 (1961) 2213.
[3] P.J. Wagner, M. Sobczak, B.-S. Park, J. Am. Chem. Soc. 120 (1998) 2488.
[4] P.K. Das, M.V. Encinas, R.D. Small Jr., J.C. Scaiano, J. Am. Chem. Soc. 101 (1979) 6965.
[5] J.C. Netto-Ferreira, V. Wintgens, J.C. Scaiano, Can. J. Chem. 72 (1994) 1565.
[6] K.C. Nicolaou, D.L.F. Gray, J. Tae, J. Am. Chem. Soc. 126 (2004) 613.
[7] K.C. Nicolaou, D.L.F. Gray, J. Am. Chem. Soc. 126 (2004) 607.
[8] D.S. Tyson, F. Ilhan, M.A.B. Meador, D.D. Smith, D.A. Scheiman, M.A. Meador, Macromolecules 38 (2005) 3638.
[9] F. Ilhan, D.S. Tyson, D.J. Stasko, K. Kirschbaum, M.A. Meador, J. Am. Chem. Soc. 128 (2006) 702.
[10] T. Tsuno, K. Sugiyama, Heterocycles 38 (1994) 859.
[11] M. Sobczak, P.J. Wagner, Tetrahedron Lett. 39 (1998) 2523.
[12] K.R. Huffman, M. Loy, E.F. Ullman, J. Am. Chem. Soc. 87 (1965) 5417.
[13] V. Lokshin, M. Valès, A. Samat, G. Pèpe, A. Metelitsa, V. Khodorkovsky, Chem. Commun. (2003) 2080.
[14] M. Valès, V. Lokshin, G. Pepe, A. Samat, R. Guglielmetti, Synthesis (2001) 2419.
[15] M. Valès, V. Lokshin, G. Pèpe, R. Guglielmetti, A. Samat, Tetrahedron 58 (2002) 8543.
[16] N.A. Larina, V. Lokshin, O. A. Fedorova, V. Khodorkovsky, to be published.
[17] M.J. Frisch, et al., Gaussian 03, Revision B. 05, Gaussian, Inc., Pittsburgh, PA, 2003.
[18] R.G. Parr, W. Yang, Density-Functional Theory of Atoms and Molecules, Oxford University Press, Oxford, 1989.
[19] J. Jaumot, R. Gargallo, A. de Juan, R. Tauler, Chemom. Intell. Lab. Syst. 76 (2005) 101.
[20] J. Hirano, K. Hamase, K. Zaitsu, Tetrahedron 62 (2006) 10065.
[21] J.J. Markham, Rev. Mod. Phys. 31 (1959) 956.
[22] B. Henderson, G.F. Inbusch, Optical Spectroscopy of Inorganic Solids, Oxford University Press, Oxford, 1989 (Chapter 5).
[23] M. Sigalov, A. Vashchenko, V. Khodorkovsky, J. Org. Chem. 70 (2005) 92.
[24] W.A. Henderson Jr., E.F. Ullman, J. Am. Chem. Soc. 87 (1965) 5424.
[25] J. Berthet, V. Lokshin, M. Valès, A. Samat, G. Vermeersch, S. Delbaere, Tetrahedron Lett. 46 (2005) 6319.
[26] J. Berthet, J.C. Micheau, G. Vermeersch, S. Delbaere, Tetrahedron Lett. 47 (2006) 2485.
[27] M. Garrido, F.X. Rius, M.S. Larrechi, Anal. Bioanal. Chem. 390 (2008) 2059.
[28] S. Aloïse, J. Réhault, B. Moine, O. Poizat, G. Buntinx, V. Lokshin, M. Valès, A. Samat, J. Phys. Chem. A 111 (2007) 1737.